Measurement of visco-elastic properties of breast-tissue mimicking materials using diffusing wave spectroscopy

C. Usha Devi
R. Sreekumari Bharat Chandran
R. Mohan Vasu
Indian Institute of Science
Department of Instrumentation
Bangalore 560 012, India

Ajay K. Sood
Indian Institute of Science
Department of Physics
Bangalore 560 012, India

Abstract. Diffusing wave spectroscopy (DWS), without the use of tracer particles, has been used to study the internal dynamics of polyvinyl alcohol (PVA) phantoms, which mimic the properties of normal and malignant breast tissues. From the measured intensity autocorrelations, the mean square displacement (MSD) of phantom meshing is estimated, leading to the storage and loss moduli of the medium covering frequencies up to 10 KHz. These are verified with independent measurements from a dynamic mechanical analyzer (DMA) at low frequencies. We thus prove the usefulness of DWS to extract visco-elastic properties of the phantom and its possible application in detecting malignancy in soft tissues. [DOI: 10.1117/1.2743081]

Keywords: diffusing wave spectroscopy; breast tissue; visco-elastic modulus; PVA phantom.

Paper 06202R received Aug. 6, 2006; revised manuscript received Dec. 5, 2006; accepted for publication Feb. 22, 2007; published online May 25, 2007.

1 Introduction

Pathological changes in soft-tissue organs are generally correlated with changes in their mechanical properties, which help to detect diseases like cancer in them. Soft tissues are visco-elastic in nature and their mechanical behavior is described by a frequency-dependent complex shear modulus $G^*(\omega)$, which has a real part $G'(\omega)$, the elastic (storage) modulus, and an imaginary part $G''(\omega)$, the viscous (loss) modulus.[1,2] A number of techniques have been developed in the past for quantitative assessment of visco-elastic properties of different kinds of materials in the context of different applications, including biomedical imaging. Elastography has come to be established as a diagnostic tool for detection of malignancy based on noninvasive measurement of tissue elastic properties.[3,4] Outside the purview of biomedical applications, visco-elastic property assessment has found a number of applications in the study of polymer solutions and gels, complex fluids and mixing of fluids, quality assessment of dairy products, etc.[1,2,5–9] Ultrasound is generally used in elastography for measuring displacement. But there are also recent developments where light is used as a probe for displacement measurement, for example, in the optical-coherence-tomography-based elastography system.[10] Diffusing wave spectroscopy (DWS), which is also used to measure visco-elastic properties of liquids and gel-like substances, has provided another light-based method for the noninvasive measurement of displacement in such media.[11,12] Such measurement of visco-elastic properties using DWS is referred to as application of DWS in microrheology.[13] Here the DWS is used to measure the mean square displacement (MSD) of the externally introduced tracer particles (usually in fluids, but also in gels) undergoing Brownian motion because of thermal fluctuations.[1,2,5–9]

In this work, we use the DWS to probe tissue-mimicking PVA phantoms to extract their visco-elastic properties. Since the ultimate targeted application is tissue imaging, the reason for using the PVA phantom in this initial study is the following: the soft tissue mainly consists of collagen, which is an elastic material, and its other constituents are elastin, reticulin, and the hydrophilic gel. The collagen fibers are interconnected with cells and intercellular substances. Thus effectively the tissue can be considered as a gel, which shows forth visco-elastic behavior quite similar to the PVA phantom used in this study.[14]

Because, a practical employment of DWS for assessing the visco-elastic properties of tissues, tracer particles have no place, we have also avoided the use of tracer particles here, their role of diffusing light being played by localized aggregates formed by physical cross-linking of polymer chains in the phantom itself. (Various types of tissues are themselves characterized by distributions of scattering centers formed by fat globules, mitochondria, etc.) DWS is based on measurement of time autocorrelation function of light that is multiply scattered in a turbid medium.[11,12] From this autocorrelation function the MSD is estimated, which in turn is used for the computation of the storage and loss moduli of the medium studied. Important features of DWS are high sensitivity to very small displacements of the scattering particles and ability to track particle dynamics, even deep inside the sample.

The conventional measurement of bulk visco-elastic properties involves the application of an external force and measurement of the resulting displacement. These methods usu-

Address all correspondence to R. M. Vasu, Instrumentation, Indian Inst. of Science, C. V. Raman Avenue, Bangalore, Karnataka 560012 India; Tel: 91 80 2293 2889; Fax: 91 80 2360 0135; E-mail: vasu@isu.iisc.ernet.in

1083-3668/2007/12(3)/034035/5/$25.00 © 2007 SPIE

ally provide frequency-dependent visco-elastic properties up to several tens of hertz only, whereas the DWS-based method can, in principle, measure these properties, even up to several megahertz. Application of external force is less preferred in medical applications done *in vivo*, which can produce substantial strains and nonlinear responses, whereas thermal excitation results in low strains and a linear response. The dynamics of the polymer mesh can be quantified by its MSD, which is obtained by DWS when multiple scattering is dominant. In many cases of abnormalities in tissue, despite the difference in mechanical properties, the small size of pathological lesions and their location deep in the body make its detection difficult and error prone when sensors are used outside the body. But DWS, as we demonstrate here, has the potential to make quantitatively accurate measurement of average visco-elastic properties of parts of an object deep within.

An outline of the work presented is as follows. Section 2 gives the theoretical framework of DWS with emphasis on application to mechanical property estimation. Section 3 describes the experiments done on the PVA phantom. Details of the data gathering and the fabrication of the phantom are also given here, as well as analysis of data and extraction of rheological properties from them. Section 4 discusses the results, and Sec. 5 puts forth the concluding remarks.

2 Theory

DWS is an extension of dynamic light scattering to study particle dynamics in highly scattering objects. With DWS it is possible to study thermally induced particle dynamics at a length scale unattainable by any of the conventional methods. The quantity measured in DWS is the temporal autocorrelation function of exiting light from which the mean square displacement (MSD) of particles is estimated. From the MSD, the complex shear modulus $G^*(\omega)$ of the surrounding medium is estimated. The normalized intensity and field autocorrelation functions, $g_2(\tau)$ and $g_1(\tau)$, respectively, are given by[11,12]

$$g_2(\tau) = \frac{\langle I(t)I(t+\tau)\rangle}{\langle I\rangle^2}, \tag{1}$$

$$g_1(\tau) = \frac{\langle E(t)E^*(t+\tau)\rangle}{\langle |E|\rangle^2}, \tag{2}$$

where $I(t)$ is the intensity of the scattered light, $E(t)$ is the complex electric field associated with the scattered light, and τ is the time shift often referred to as the delay time. Here the angular brackets indicate time averaging.

Assuming the electric field to be a Gaussian random variable, $g_2(\tau)$ and $g_1(\tau)$ are related through the Siegert relation[11] $g_2(\tau)=1+f|g_1(\tau)|^2$, where f is a factor dependent on the collection optics used in the experiments. In DWS using transmission geometry, $g_1(\tau)$ is inverted to get MSD $\langle\Delta r^2(\tau)\rangle$, using the so-called zero crossing routine.[12] The MSD is related to $g_1(\tau)$ through[12,15]

$$g_1(\tau) = \exp\left[-\left(\frac{L}{\ell^*}\right)^2 k_0^2\langle\Delta r^2(\tau)\rangle\right]. \tag{3}$$

Here k_0 is the modulus of the optical wave vector, L is the thickness of the sample, and ℓ^* is the transport mean-free path length of photons in the object. The MSD reflects the response of the material to the stress experienced by it by the thermal fluctuations. Using MSD, the full frequency-dependent visco-elastic moduli $G^*(\omega)$ can be estimated as,[1]

$$G^*(\omega) = \frac{k_B T}{\pi\xi i\omega F\{\langle\Delta r^2(\tau)\rangle\}}. \tag{4}$$

Here ξ is the mean particle size in the object, k_B and T are the Boltzmann constant and absolute temperature, respectively, and $F\{\langle\Delta r^2(\tau)\rangle\}$ is the Fourier transform of the MSD.

The storage modulus $G'(\omega)$ and the loss modulus $G''(\omega)$ are obtained by[1,2]

$$G'(\omega) = G(\omega)1/[1+\beta'(\omega)] \times\cos\left[\frac{\pi\alpha'(\omega)}{2} - \beta'(\omega)\alpha'(\omega)(\pi/2-1)\right], \tag{5}$$

$$G''(\omega) = G(\omega)1/[1+\beta'(\omega)]\sin\left[\frac{\pi\alpha'(\omega)}{2} - \beta'(\omega)[1-\alpha'(\omega)] \times(\pi/2-1)\right], \tag{6}$$

where

$$G(\omega) = \frac{k_B T}{\pi\xi\langle\Delta r^2(1/\omega)\rangle\Gamma[1+\alpha(\omega)][1+\beta(\omega)/2]}. \tag{7}$$

Here $\alpha(\omega)$ and $\beta(\omega)$ are the first- and second-order logarithmic time derivatives of the MSD ($\langle\Delta r^2(\tau)\rangle$) data, respectively, $\langle\Delta r^2(1/\omega)\rangle$ is the magnitude of $\langle\Delta r^2(\tau)\rangle$ evaluated at $\tau=1/\omega$, Γ denotes the gamma function, and $\alpha'(\omega)$ and $\beta'(\omega)$ are the first- and second-order logarithmic derivatives of $G(\omega)$, respectively.

The process of physical cross-linking of molecules of aqueous PVA, which form flexible chains, results in the formation of PVA gel used here, and the density of cross-links is controlled by the method of preparation.[16] In the PVA gel, the aggregates formed by the network of flexible chains serve as scattering centers and therefore the average particle size describes the average spacing between chains or size of voids between the filaments. The particle size (ξ) in Eq. (7) is taken to be the characteristic mesh size of the polymer network.

Network structures are usually characterized in terms of cross-linking density ρ, the average molecular weight between cross-links M_e, and mesh size ξ. The mesh size ξ of the PVA gel can be evaluated,[17] under the approximation that the chains of networks are in *Gaussian conformational regime*, through the equation,[17,18]

$$\xi = \phi_2^{-1/3}(C_\infty M_e/\langle M_r\rangle)^{1/2} l. \tag{8}$$

Here $\langle M_r\rangle$ is the mass of average repeating unit between two cross-links, C_∞ is the *characteristic ratio* of the PVA chain

with a carbon-carbon bond length l, and ϕ_2 is the polymer volume fraction of the network after swelling. In the case of the PVA gel we have fabricated, the values of the parameters needed (M_e, $\langle M_r \rangle$, and ϕ_2) are not yet estimated and therefore the mesh size was not determined through this route.

For a densely cross-linked polymer gel, ξ is also the typical distance between cross-links from which the storage modulus $G'_{\omega=0}$ can be found through

$$G' = k_B T \xi^{-3}. \quad (9)$$

We have estimated the mesh size by experimentally determining the elastic modulus through a low frequency sweep measurement using the DMA and Eq. (9).

3 Experimental System

3.1 *Preparation Characterization of Polyvinyl Alcohol Phantoms*

The PVA hydrogel is created from PVA stock with different degrees of hydrolysis[16] by promoting cross-linking between the polymer filaments, which enhances its mechanical strength. The cross-linking is enhanced by subjecting the PVA solution to repeated freezing-thawing cycles.[16] Apart from promoting cross-linking of filaments, the freeze-thaw cycles also create a number of voids in the gel, which enhance light scattering, giving the gel a scattering coefficient comparable to that of certain tissue samples. We have produced a number of PVA gel samples of varying mechanical strength and scattering coefficients by subjecting PVA solutions of different degrees of hydrolysis to suitable numbers of freeze-thaw cycles.

Starting from 98% hydrolysis PVA stock solution by increasing the number of freeze-thaw cycles from 2 to 7, we produced samples of PVA gels with storage modulus increasing from 11.4 to 97.3 kPa. The corresponding increase in reduced scattering coefficient was from 0.159 to 0.495 mm^{-1}. With 99% hydrolysis PVA stock solution, the corresponding values of storage modulus and reduced scattering coefficients varied from 65.5 to 149.0 kPa and 0.253 to 0.445 mm^{-1}, respectively. Using this method, we have fabricated a number of PVA gel samples whose storage modulus values were tailored to high or low values as desired.

3.2 *Measurement of Intensity Autocorrelation of Transmitted Light through the Phantom Samples*

The experimental setup to measure $g_2(\tau)$ of light transmitted through the sample is shown schematically in Fig. 1. Light from a He–Ne laser ($\lambda = 632.8$ nm) is sent through the sample, which is a rectangular slab of PVA gel (thickness varying from 24 to 12 mm for different phantoms) sandwiched to a cell containing an ergodic medium like suspensions of polystyrene beads in glycerol. The reason for the use of this double cell and the way $g_2(\tau)$ of the gel is extracted from the combined $g_2(\tau)$'s measured for the double cell and the ergodic medium are explained later in this section. The multiple-scattered light exiting the medium forms a speckle pattern, and light from a single speckle is gathered by a single-mode fiber and given to a photon-counting head, which

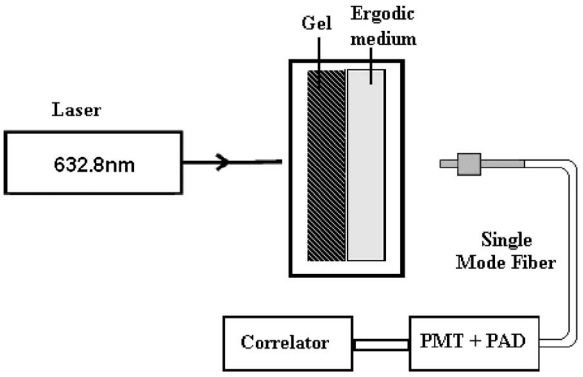

Fig. 1 Schematic representation of the DWS experimental setup in the transmission geometry. The double-cell setup compensates for the nonergodic behavior of the gel. The first sample is the PVA phantom and the second is a quartz cell containing a suspension of polystyrene beads of 1 μm diam in glycerol (1% solution) for which $L_2/\ell_2^* = 5$. The solid phantom is sandwiched tightly to the cell, and leakage of light, if any, is minimal.

is integrated equipment consisting of a PMT, a pulse amplifier discriminator (PAD), and a correlator. The correlator gives the intensity autocorrelation of the detected light.

Our PVA phantom is a gel-like substance and exhibits nonergodic behavior. On the other hand, the double cell with a sandwich of the gel and the ergodic sample displays ergodic behavior.[18] Light on its way from the source to the detector interacts first with the gel sample of thickness L_1 and then with the ergodic medium of thickness L_2, consisting of a 1% volume fraction of 1.0-μm polystyrene balls in glycerol with moderate scattering coefficient. The sample thickness is selected such that optical density for phantom L_1/ℓ_1^*, varied from 4.5 to 5 (for different samples) and $L_2/\ell_2^* = 5$ for the ergodic medium, so that the sample is symmetric and the multiplication rule can be applied (here ℓ_1^* and ℓ_2^* are the transport mean free pathlengths for the gel and the ergodic sample, respectively). We calculate the intensity autocorrelation for the gel $[g_2(\tau, L_1)]$ from the measured $g_2(\tau, L_1 L_2)$ and $g_2(\tau, L_2)$, measured separately for the ergodic medium alone, using the relation[19]

$$g_2(\tau, L_1 L_2) - 1 = [g_2(\tau, L_1) - 1][g_2(\tau, L_2) - 1]. \quad (10)$$

Typical intensity autocorrelation functions measured from the double-cell experiment, one corresponding to the sandwich and the other for the ergodic sample alone, are shown in Fig. 2(a). From a set of these measurements, the average intensity autocorrelation function corresponding to a number of phantom samples (storage modulus values 11.4, 23.4, and 40.4 kPa) were calculated. From the measured intensity autocorrelations, the field autocorrelations and the MSD data are obtained using Eq. (3) and the already measured ℓ^* values of the phantom. A second-order polynomial fit using a sliding Gaussian window[1,2] is used to smooth the MSD data and to obtain $\alpha(\omega)$ and $\beta(\omega)$. These are used to arrive at $G(\omega)$ using Eq. (7) and hence to calculate $\alpha'(\omega)$ and $\beta'(\omega)$ by taking the first- and second-order logarithmic derivatives of $G(\omega)$. Then the moduli $G'(\omega)$ and $G''(\omega)$ are obtained using Eqs. (5) and (6).

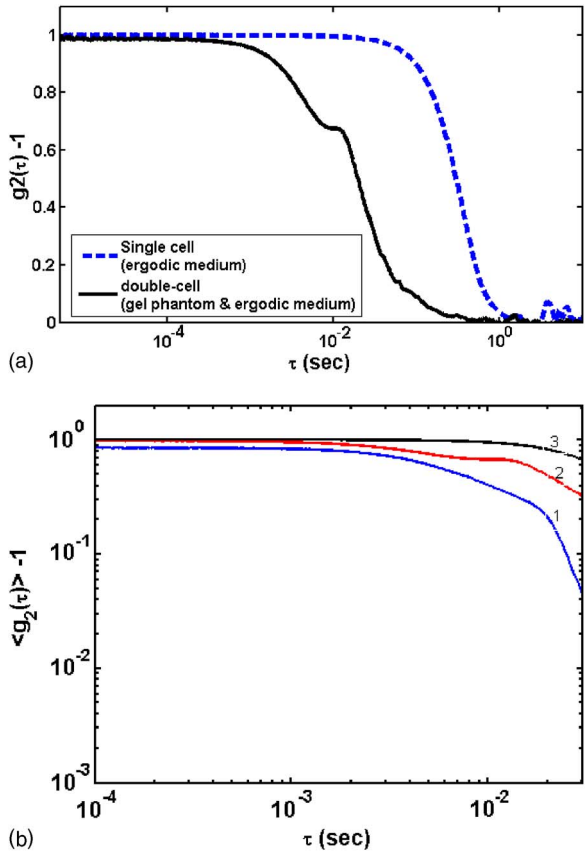

Fig. 2 (a) Typical intensity autocorrelation for the ergodic $[g_2(\tau, L_2) - 1]$ as well as the sandwich $[g_2(\tau, L_1 L_2) - 1]$ of two media, from which $g_2(\tau, L_1) - 1$ is extracted. The solid line shows the $g_2(\tau, L_2) - 1$ with respect to time, and the dotted line represents $g_2(\tau, L_1 L_2) - 1$. (b) Intensity autocorrelation $g_2(\tau, L_1) - 1$ extracted from the data of (a) for different phantoms with increasing elastic moduli: 11.4 kPa (line 1), 23.4 kPa (line 2), and 40.4 kPa (line 3).

3.3 *Estimation of the Characteristic Mesh Size (ξ) of Polyvinyl Alcohol Samples*

Use of Eqs. (5) and (6) to estimate $G'(\omega)$ and $G''(\omega)$ requires the parameter ξ, apart from the MSD and other parameters derivable from the MSD. In polymer materials, this parameter is usually estimated from the plateau modulus, which depends on a characteristic molecular weight (M_e) called molecular weight between cross-links, as explained in Sec. 2. For polymers, which belong to the same family as PVA, the values of M_e are available in the literature from which ξ can be determined.[17] For the PVA gel used in our experiment, M_e is not yet estimated (to the best of our knowledge). Therefore we did not estimate ξ here following this route, and instead resorted to an experimental shortcut to get ξ. However, ξ should be determined using Eq. (8), to make the present study useful to estimate elastic property from practical DWS measurements of $g_2(\tau)$.

We have performed mechanical measurements (low frequency sweep) using the DMA (Eplexor 500N from GABO Qualimeter Testanlagen GmbH, Ahlden/Germany) to determine the frequency-dependent storage dynamic (or complex) modulus $[G^*(\omega)]$ by subjecting the samples to periodic stress, and measuring the resulting strain. This method gives $G'(\omega)$ and $G''(\omega)$ for frequencies up to 100 Hz. We used one of these measurements of $G'(\omega)$ at the lowest frequency, in Eq. (9), to recover ξ. The ξ so obtained is the average mesh size for the PVA phantom, and the values we obtained through this are 6.6, 5.0, and 4.6 nm, corresponding to storage modulus values of 11.4, 23.4, and 40.4 kPa, respectively. These values are comparable to the ξ values for materials such as polystyrene and polyethylene (8.2 and 3.4 nm, respectively, which are concentration dependent) for which independent estimates through theoretical means are available.[17]

The low frequency measurements of $G'(\omega)$ and $G''(\omega)$ obtained using DMA are also employed in verifying the measurements from the DWS experiment. This is further touched on in Sec. 4, where the measurement results are discussed.

4 Results and Discussions

Figure 2(a) shows intensity autocorrelations $g_2(\tau)$-1 plotted against time, for the ergodic sample and for the combined medium, for a typical case (elastic storage modulus of phantom is 23.4 kPa), which helps us see that the time scale of relaxation in the ergodic medium and the sandwich are comparable. The intensity autocorrelations $g_2(\tau, L_1)$-1 for different samples, extracted from the double-cell measurements applying the multiplication rule, are shown in Fig. 2(b).

The storage and loss modulus estimated from $g_2(\tau)$, following the procedure described in the previous section, are plotted in Figs. 3(a) and 3(b). The DWS-based method resulted in $G'(\omega)$ and $G''(\omega)$ extending from $\omega = 50$ to 10 kHz. The lower frequency limit was because of the fact that $g_2(\tau)$ for the sample was extracted from measurement from the sandwich of the sample and an ergodic medium as described earlier. And from the ergodic medium with suspended particle of size of 1 μm, $g_2(\tau)$ cannot be accurately estimated beyond $\tau = 0.02$ s. The $G'(\omega)$ measured from three PVA samples of storage moduli 11.39, 23.42, and 40.35 kPa are shown in Fig. 3(a) with ω varying from 50 to 10 kHz. For comparison, the measurements using the DMA for a range of frequencies from 1 to 100 Hz are also shown. Figure 3(b) is similar plots of loss moduli $G''(\omega)$ for the three samples. It is seen that the agreement in small frequency range from 50 to 100 Hz, where there is an overlap in the frequency range possible from the two sets of measurements, is excellent. The loss modulus measured, for the higher stiffness phantom, from the $g_2(\tau)$ shows an upward trend with frequency.

5 Conclusions

We experimentally demonstrate the application of a DWS-based method for extracting the visco-elastic properties of tissue-property mimicking PVA phantoms. The loss and storage moduli are measured in a wide frequency range, starting from 50 to ~10 kHz. The novelty here is that the usual tracer particles used in the microrheology experiments with DWS are dispensed with, their role being played by filament aggregates in the polymer. Verification of these measurements in a smaller low-frequency range (50 to 100 Hz) is done by comparison with measurements obtained from a mechanical analyzer. The formula used to convert $g_2(\tau)$ measured to storage and loss moduli involves a parameter ξ, the average mesh

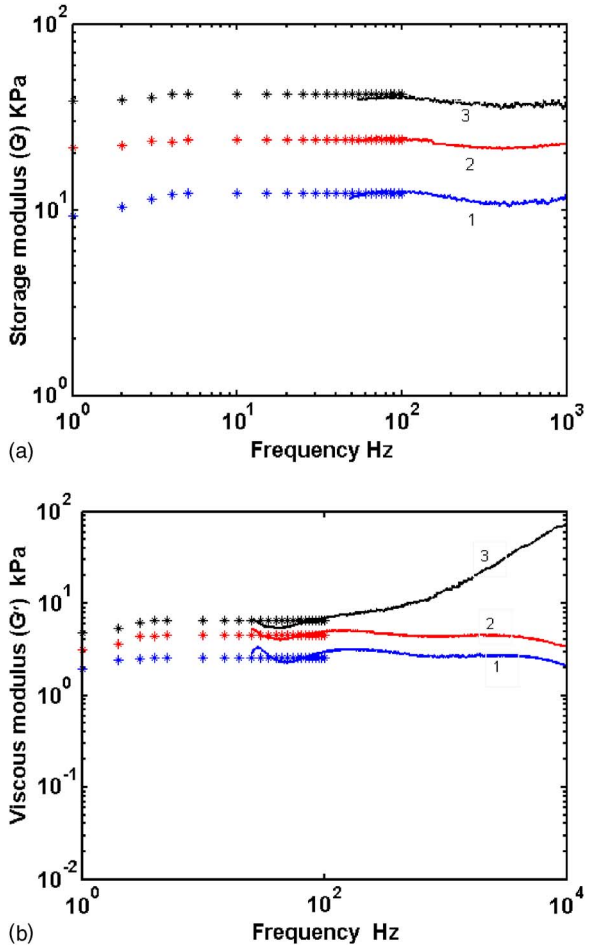

Fig. 3 (a) Comparison of the measured frequency-dependent elastic moduli of PVA phantoms obtained from the DWS experiments (solid lines) with those from the mechanical analyzer (symbols). From the DWS, the measurements are obtained in the frequency range from 50 Hz to 10 kHz, whereas from the DMA the range is from 1 to 100 Hz. The average storage modulus measured by the DMA for the three phantom samples are: line 1, 11.4; line 2, 23.4; and line 3 40.4, in kPa. (b) The same as in (a), except that here the viscous moduli are compared. The average viscous modulus measured by the DMA for the three phantom samples are: line 1, 2.52; line 2, 4.35; and line 3, 6.1, in kPa.

size of the polymer. There are standard theoretical methods for finding ξ, which have already been used to extract the mesh size of polymers in the same family as PVA. These are not yet applied for the PVA phantom used here. Either these or experimental methods based on ultrasound[20,21] should be established to get the distribution of mesh size ascertained, so that the method suggested in this study can be applied in practice without the need for a convoluted measurement of mesh size from the storage modulus.

The present method measures the average visco-elastic properties of the samples. To extend this method to image visco-elastic property in an inhomogeneous object, the propagation of field correlation through the object has to be modeled. Such models are available,[22] and the solution of an associated inverse problem can result in the map of the distribution of the storage and loss moduli of the material.

References

1. B. R. Dasgupta, S. Y. Tee, J. C. Crocker, B. J. Frisken, and D. A. Weitz, "Microrheology of polyethelene oxide using diffusing wave spectroscopy and single scattering," *Phys. Rev. E* **65**, 051505 (2002).
2. B. R. Dasgupta and D. A. Weitz, "Microrheology of cross linked polyacrylamide networks," *Phys. Rev. E* **71**, 021504 (2005).
3. J. F. Greenleaf, M. Fatemi, and M. F. Insana, "Selected methods for imaging elastic properties of biological tissues," *Annu. Rev. Biomed. Eng.* **5**, 57 (2003).
4. T. Varghese and T. J. Hall, "Visco-elastic characterization of in vitro canine tissue," *Phys. Med. Biol.* **49**, 4207 (2004).
5. H. M. Wyss, S. Romer, F. Scheffold, P. Schurtenberger, and L. J. Gauckle, "Diffusing wave spectroscopy of concentrated Alumina suspensions during gelation," *J. Colloid Interface Sci.* **240**, 89 (2001).
6. A. Palmer, T. G. Mason, J. Xu, S. C. Kuo, and D. Wirtz, "Diffusing wave spectroscopy microrheology of actin filament networks," *Biophys. J.* **76**, 1063 (1999).
7. T. G. Mason, H. Gang, and D. A. Weitz, "Diffusing-wave spectroscopy measurements of visco-elasticity of complex fluids," *J. Opt. Soc. Am. A* **14**(1), 139 (1997).
8. L. F. Rojas, R. Vavrin, C. Urban, J. Kohlbrecher, A. Stradner, F. Scheffold, and P. Schurtenberger, "Particle dynamics in concentrated colloidal suspensions," *Faraday Discuss.* **123**, 385 (2003).
9. M. Alexander and D. G. Dalgleish, "Application of transmission diffusing wave spectroscopy to the study of gelation of milk by acidification and rennet," *Colloids Surf., B* **38**, 83 (2004).
10. M. J. Schmitt, "OCT elastography: Imaging microscopic deformation and strain of tissue," *Opt. Express* **3**, 119–211 (1999).
11. G. Maret, "Diffusing wave spectroscopy," *Curr. Opin. Colloid Interface Sci.* **2**, 251 (1997).
12. D. A. Weitz and D. J. Pine, "Diffusing wave spectroscopy," in *Dynamic Light Scattering: The Method and Some Applications*, W. Brown, Ed., Oxford University Press, Oxford, UK (1993).
13. C. MacKintosh and C. F. Schmidt, "Microrheology," *Curr. Opin. Colloid Interface Sci.* **4**, 300 (1999).
14. Y. C. Fung, "Bio-viscoelastic solids," Chap. 7 in *Biomechanics: Mechanical Properties of Living Tissues*, p. 196, Springer Verlag, New York (1981).
15. N. Menon and D. J. Durian, "Diffusing wave spectroscopy of dynamics in a three dimensional granular flow," *Science* **275**, 1920 (1997).
16. C. Usha Devi, R. M. Vasu, and A. K. Sood, "Design, fabrication and characterization of tissue-equivalent phantom for optical elastography," *J. Biomed. Opt.* **10**(4), 044020(1) (2005).
17. G. Paradossi, F. Cavalieri, E. Chiessi, and M. T. F. Telling, "Supercooled water in PVA matrixes: I. An incoherent quasi-elastic neutron scattering (QENS) Study," *J. Phys. Chem.* **107**, 8363–8371 (2003).
18. M. Doi and S. F. Edwards, *Theory of Polymer Dynamics*, Clarendon Press, Oxford, UK (1986).
19. F. Scheffold, S. E. Skipetrov, S. Romer, and P. Schurtenberger, "Diffusing wave spectroscopy of nonergodic media," *Phys. Rev. E* **63**, 061404 (2001).
20. M. F. Insana and T. J. Hall "Characterising the microstructure in the random media using ultrasound," *Phys. Med. Biol.* **35**(10), 1373 (1990).
21. T. A. Bigelow, and W. D. O'Brien, Jr., "Scatterer size estimation in pulse-echo ultrasound using focused sources: Theoretical approximation and simulation analysis," *J. Acoust. Soc. Am.* **116**, 578 (2004).
22. D. A. Boas, L. E. Campbell, and A. G. Yodh, "Scattering and imaging with diffusing temporal field correlations," *Phys. Rev. Lett.* **75**, 1855 (1995).